Volume 12, Number 1, 2019. pp. 87-96

Jordan Journal of Physics

ARTICLE

Effect of Relaxation and Cooling Process on Field Electron Emission from Single-Walled Carbon Nanotubes Embedded in Glass

Marwan S. Mousa and **Samer I. Daradkeh**

Surface Physics and Materials Technology Lab. Department of Physics, Mutah University, Al-Karak 61710, Jordan.

Received on: 2/7/2018; *Accepted on: 7/3/2019*

Abstract: Several experiments examined the properties of Field Electron Emission (FEE) from Single-Walled Carbon Nanotubes (SWCNTs), where extensive studies were conducted to improve the emission current density (stability and repeatability) and emission current image concentration. In this study, the effect of relaxation and cooling processes on FEE from SWCNTs embedded in glass has been investigated to keep the ongoing investigation for factors that positively affect the FEE process. It has been found that the relaxation process can ameliorate the FEE, where the "switch-on" phenomenon occurs at lower applied voltage after performing the relaxation process. Also, the saturation region extends down to lower applied voltage values after the relaxation process. In case of the effect of cooling process on FEE, the "switch-on" phenomenon occurs at higher applied voltage values after applying the cooling process. Also, the saturation region extends down to higher applied voltage values and the threshold value has been found to significantly being lowered as the result of the cooling process, where the emission current disappeared at applied voltage values of ~20 V. In terms of the effects of the cooling process on emission current images, the emission current image is distributed throughout the screen. Furthermore, it has been experiencing a massive emission current fluctuation after performing the cooling process.

Keywords: Field Electron Emission, Single-Walled Carbon Nanotubes, Relaxation and Cooling Processes.

Introduction

Field electron emission (FEE) is defined as the extraction of free electrons from the surface of a metal caused by an external energy source in the form of an applied electrostatic field [1]. This electrostatic field can bend the potential barrier, so quantum tunneling could take place through the surface potential barrier. Metals are the most commonly used field emitters. However, FEE can take place from metals, semiconductors [2-3], liquids [4] and non-conducting materials [5]. But, the most promising material that could replace metals as a field electron emitter is the Carbon Nanotube (CNT).

The excellent (FEE) features of Carbon Nanotubes (CNTs) have been investigated in several experiments, which started with Rinzler in 1995 [6] and kept going on till now [7-9]. After MWCNTs have been discovered by Sumio lijima in 1991 [10], SWCNTs by the same scientist in 1993 [11] and due to their unique properties like high aspect ratio, MWCNTs can lead to a great enhancement of the local electric field near the tip [12]. Also, those are characterized with having long-life time, being less sensitive to operating environment than metallic emitters [13] and the occurrence of field penetration that would lead to reduce the effective work function [14]. The previous properties make CNTs the best candidate to be used as field electron emitters. So, they have been used in many applications in both

Corresponding Author: Marwan S. Mousa **Email**: mmousa@mutah.edu.jo

technological and industrial fields, like micro- and nano-electronics [15], flat-panel displays [16], radar absorbing coating [17], gas storage and sensors [18]. There are many experimental tests that have been performed to study the effect of several factors on FEE from CNTs, in order to have better understanding of and control the FEE mechanism from CNTs.

The theoretical explanation of FEE has been derived by Fowler and Nordheim in 1928 [19] based on several assumptions, like assuming that the emitter is a smooth flat planar surface, with a uniform external electrostatic field F_{ext} in a vacuum above the emitter. Atomic structure has been ignored and a Sommerfeld-type free-electron model has been assumed. The electron population taken is to obey Fermi-Dirac statistics and to be in thermodynamic equilibrium at thermodynamic temperature T [20]. Also, the role of atomic wave-functions in transmission theory has been disregarded. For real-field emitters, these assumptions are unrealistic. So, the theory must be corrected and improved, in order to present a reasonable explanation and prediction of the FEE for new electron emitters, like SWCNTs.

There are research studies that have been carried out to investigate the effect of several factors on the field electron emission, such as the effect of an internally conductive coating on the electron emission from glass tips [21] and the effect of insulting layer on the field electron emission performance of Nano-Apex metallic emitters [22]. The effect of gas adsorption on the field emission of Carbon Nanotubes [23], the effect of aging on field emission lifetime for carbon nanotube cathodes [24], among others, were reported. So, it can be indicated that the field electron emission can be affected by several factors. Our research reported here aims at studying the effect of relaxation and cooling processes. For applying the relaxation process, the emitter is left overnight under high-vacuum conditions after its initial "switch-on" process [22]. The relaxation process has been found to enhance the FEE from SWCNTs. The effect of cooling process on FEE from SWCNTs embedded in micro-glass tip emitters has been investigated. The cooling process can be achieved by adding liquid nitrogen (LN_2) inside the specially designed sample holder; thus having the sample at standardized separation close to LN_2. This kind of emitter has been manufactured by employing a drawing technique using a glass puller [25], where it has been found that the cooling process affects the threshold values needed for the emission process as well as the distribution of the emission current image over the conductive phosphorus screen.

Materials and Methodology

In this paper, we will discuss the current-voltage (I-V) characteristics and the related FN plots that have been extracted from the SWCNTs. The material (SWCNTs) in our experiments was produced by catalytic conversion of high-pressure CO over Fe particles (HiPCO) processed at CNI-Huston-Texas, having an average diameter ranging between (1 - 4) nm with a length of (1 - 3) µm. The emitters were manufactured by employing a drawing technique using glass puller apparatus, that is shown in Fig. 1.

FIG. 1. Actual image of the glass puller apparatus.

The components of the glass puller apparatus were illustrated somewhere else [21]. The SWCNTs were inserted inside the glass tube using mechanical procedures, by pushing the SWCNTs all the way inside the glass tube using a tungsten wire until they reach the tip, then the emitter was positioned inside a Field Emission Microscope (FEM), where the emitter-screen distance of ~10 mm is standardized. The glass tube length was about 1 cm. The system was evacuated to a vacuum with a pressure of ~10^{-8} mbar, then the system was baked to ~170 °C overnight.

Fig. 2 shows the optical micrographs of (SWCNT-21) and (SWCNT-1) tips, where the SWCNTs are in the broken end of the glass tube opposite to the anode.

Fig. 3 shows the SEM image for (SWCNT-21) and (SWCNT-1), respectively. The tip hole diameter for SWCNT-21 is 396.5 µm and the tip hole diameter for SWCNT-1 is 246.6 µm.

As it has been previously mentioned, the relaxation process can be applied by leaving the emitter for ~12 hours under high-vacuum pressure after its initial "switch-on" phenomenon occurs. The cooling process is performed by adding liquid nitrogen inside the sample holder and leaving the system for ~5 min, until the cooling process takes effect. Fig. 4 shows how the cooling process can be performed.

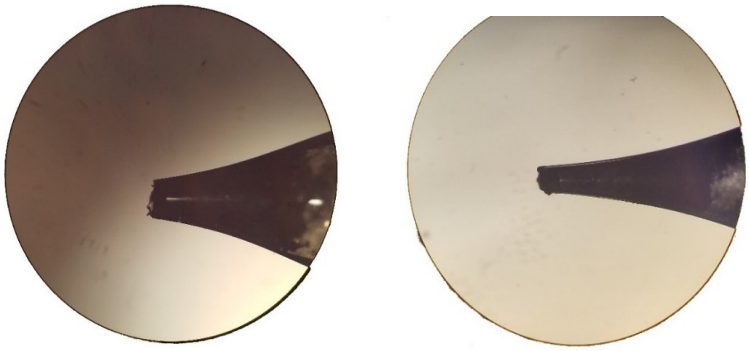

FIG. 2. Optical micrographs of (SWCNT-21) tip and (SWCNT-1) tip at a magnification of 50 times, respectively.

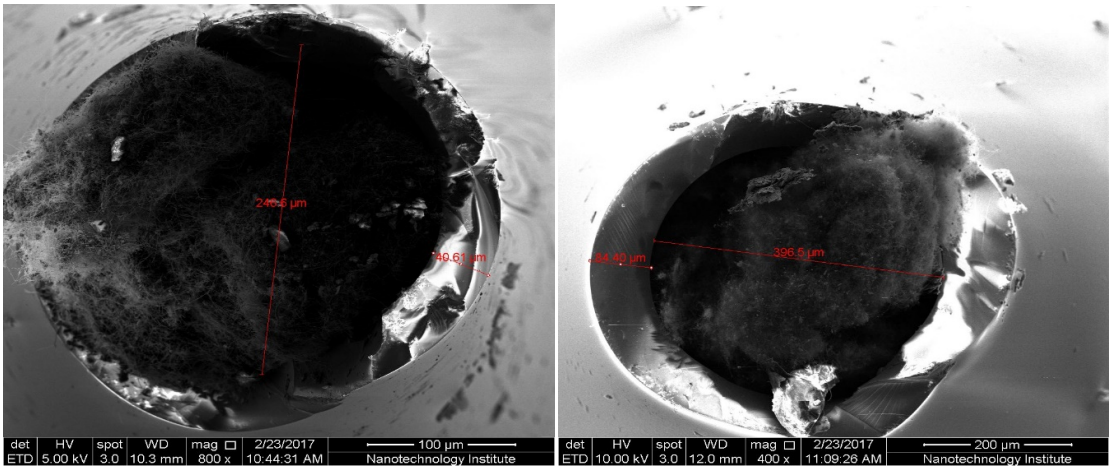

FIG. 3. SEM images of (SWCNT-21) tip at a magnification of 400 times and (SWCNT-1) tip at a magnification of 800 times, respectively.

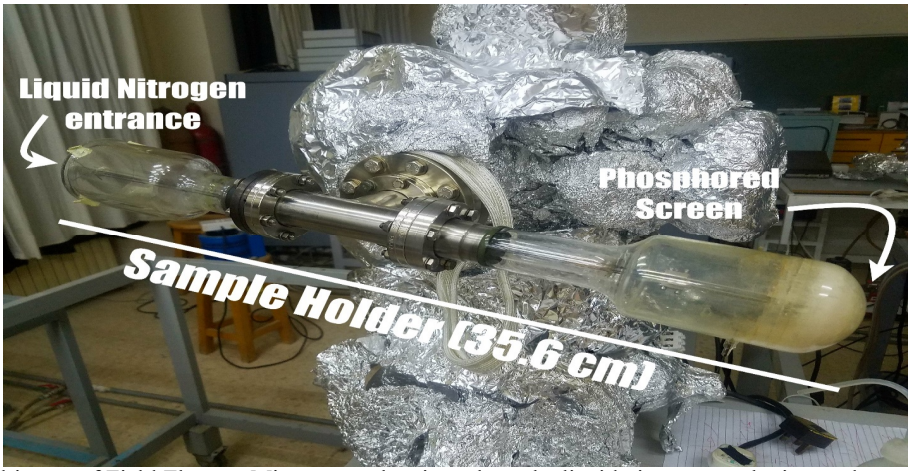

FIG. 4. Actual image of Field Electron Microscopy showing where the liquid nitrogen can be inserted to perform the cooling process.

The testing procedures start with increasing the applied voltage V slowly until the "switch-on" phenomenon V_{SW} occurs. At this point, the emission current suddenly increases from nano-ampere range to micro-ampere range. After that, the applied voltage is decreased, so the emission current will fall smoothly to zero. The threshold value V_{TH} will be measured, which is the lowest applied voltage value, at which the emission current is at its lowest value [26].

Results and Discussion

The effect of the relaxation process on FEE has been discussed based on the I-V characteristics curve and the FN plot for FEE from SWCNTs-1. Due to the increase of the applied voltage on the (SWCNT-1) tip, the emission current has been initiated with (8 pA), with an applied voltage of (600 V). By further increasing the voltage, the emission current increased until V_{SW} was reached; this occurs at (1350 V) producing an emission current of (3.7×10^3 nA). We continued increasing the applied voltage to (1730 V), where the emission current becomes (9.5×10^3 nA). After that, we started to decrease the applied voltage. The saturated region extended down to a voltage value (V_{SAT} = 1000 V), where the emission current value became (I_{SAT} = 1.21×10^3 nA). Emission current vanishes after applied voltage value (V_{TH} = 350 V) was reached, with the emission current becoming (I_{TH} = 9.45 pA). Fig. 5 shows the I-V characteristics with the related FN plot before the relaxation process and the slope of FN plot at low-emission current presented in the FN plot.

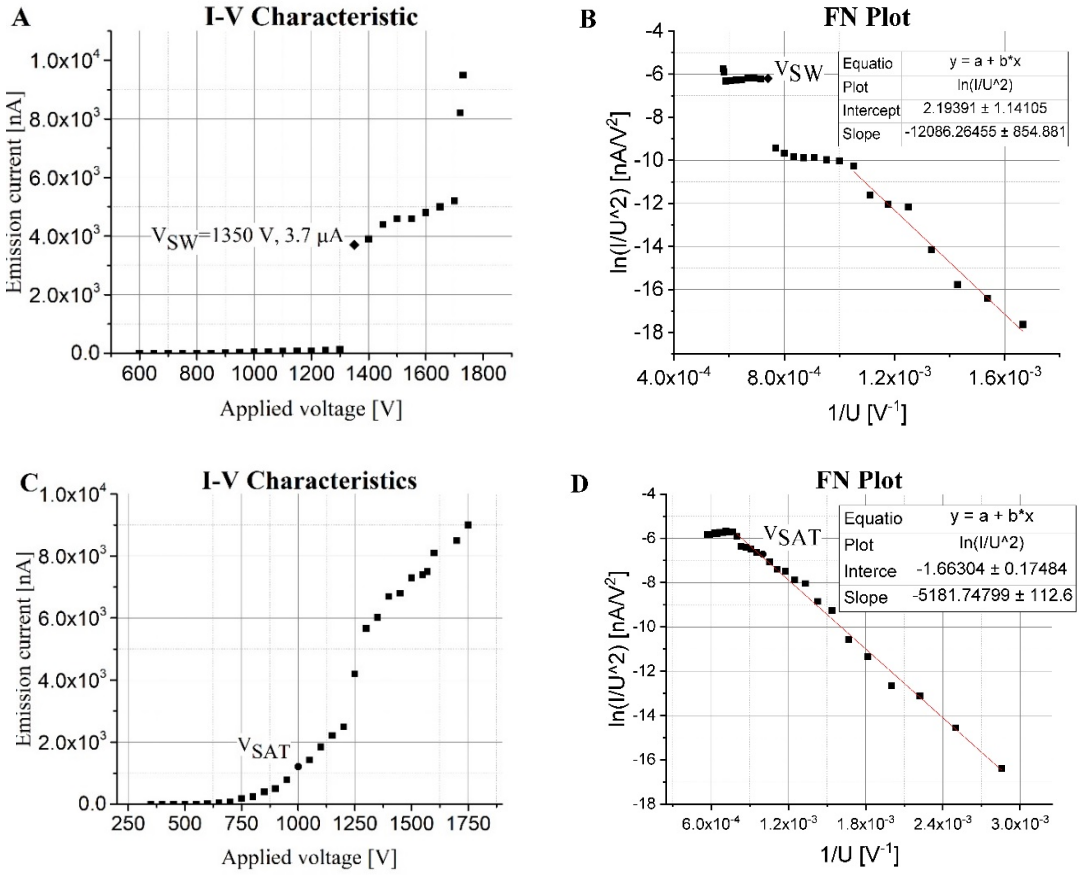

FIG. 5. Before performing the relaxation process on (SWCNT-1). At increasing voltage (A) I-V Characteristics. (B) FN plot. At decreasing voltage (C) I-V Characteristics. (D) FN plot.

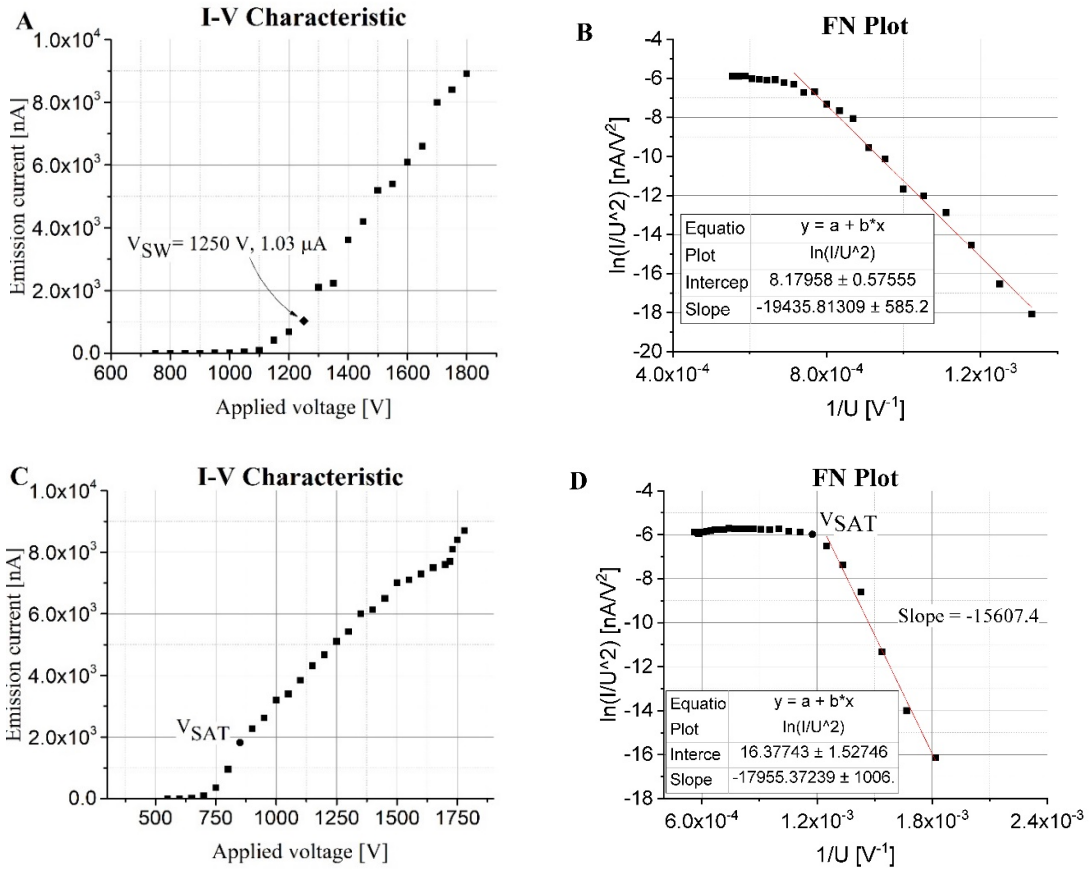

FIG. 6. (SWCNT-1).I-V characteristics and related FN plot after relaxation process. At increasing voltage: (A) I-V Characteristics. (B) FN plot with a slope of -19435.8 Np (at low emission current). At decreasing voltage: (C) I-V Characteristics. (D) FN plot with a slope of -17955.37 Np.

Fig. 5A shows an emission current that suddenly jumps from 137.2 nA at 1300 V to 3.7×10^3 nA at 1350 V, which can be attributed to the formation of a new conducting channel. Later on, the system was left for ~12 hours to study the effect of the relaxation process. After applying the relaxation process, a second cycle of increasing and decreasing of applied voltage begun with increasing the applied voltage. This voltage ranges from 750 V up to 1800 V with emission current values ranging from 8 pA up to 8.92×10^3 nA as the applied voltage increased. The switch on phenomenon occurs at a voltage value V_{SW} = 1250 V with an emission current I_{SW} = 1.03×10^3 nA, as seen in Fig. 6A. By decreasing the applied voltage, emission current decreased, but this current remained at micro-ampere range until V_{SAT} = 850 V was reached and the emission current was $I_{SAT} = 1.82\times10^3$ nA, as shown in Fig. 6C. After that point, the emission current decreased to nano-ampere range, until it vanished at (V_{TH} = 550 V, I_{TH} = 30 pA). Fig. 7 shows the emission images before and after the relaxation process.

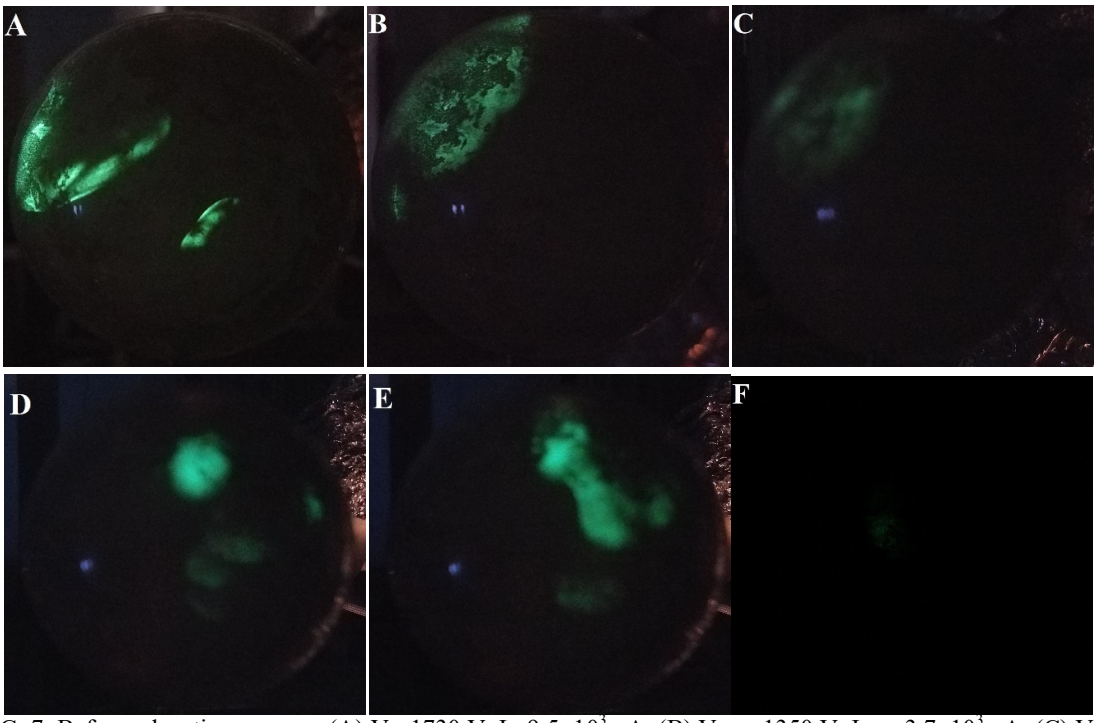

FIG. 7. Before relaxation process: (A) V =1730 V, I =9.5×10^3 nA. (B) V_{SW} =1350 V, I_{SW} =3.7×10^3 nA. (C) V = 1300 V, I = 0.137×10^3 nA. After relaxation process: (D) V =1800 V, I =8.92 μA. (E) V_{SW} =1730 V, I_{SW} = 8.1×10^3 nA. (F) V = 1200 V, I =0.68×10^3 nA.

The linear behavior that appears at the I-V characteristics in Fig. (6-A and C) can be an indication of the existence of a constant resistance somewhere at the CNT/substrate interface or along the CNT [27], or as an effect of space charge, where it can suppress the FEE from the SWCNT emitter [28].

By comparing Fig. 5 with Fig. 6, it can be noticed that there is an improvement in the shape of plots (both I-V characteristics and FN plots). It is obvious that the relaxation process made the emission current pattern more concentrated based on comparing the emission current pattern before and after the relaxation process as shown in Fig. 6. Figs. (7 A, B and C) represent the emission current images before the relaxation process, where it can be seen from these images that the emission current images are not concentrated. Figs. (7 D, E and F) are the emission current images after the relaxation process and it can be inferred from these figures that the relaxation process affects the emission current images' concentration pattern.

The effect of the cooling process on FEE has been discussed based on the I-V characteristics curve and the FN plot for FEE from SWCNT-21. Cooling process can be achieved by adding liquid nitrogen inside the sample holder and leaving the system for ~15 min, so cooling can have its effect on the sample. Before applying the cooling process, the emission current initiated at an applied voltage value of 320 V, where the emission current was 4.2 pA. With slowly increasing of the applied voltage, the emission current gets increased until a sudden jump happens in the emission current, where it is increased from 80.3 nA to I_{SW} = 3.05×10^3 nA, where the applied voltage value was V_{SW} = 700 V. Afterwards, we continued increasing the applied voltage until it reached 1050 V, where the emission current was 6.2×10^3 nA. By decreasing the applied voltage, the saturation region extends down to V_{SAT} = 450 V and I_{SAT} = 1.1×10^3 nA. By further decreasing the applied voltage, the emission current decreased until it vanishes at (V_{TH} = 140 V, I_{TH} = 4.2 pA) (see Fig. 8). It should be noted that the slope before the cooling process, during increasing and decreasing the applied voltage, has values of (-5297.5 Np) and (-2347.78 Np), respectively.

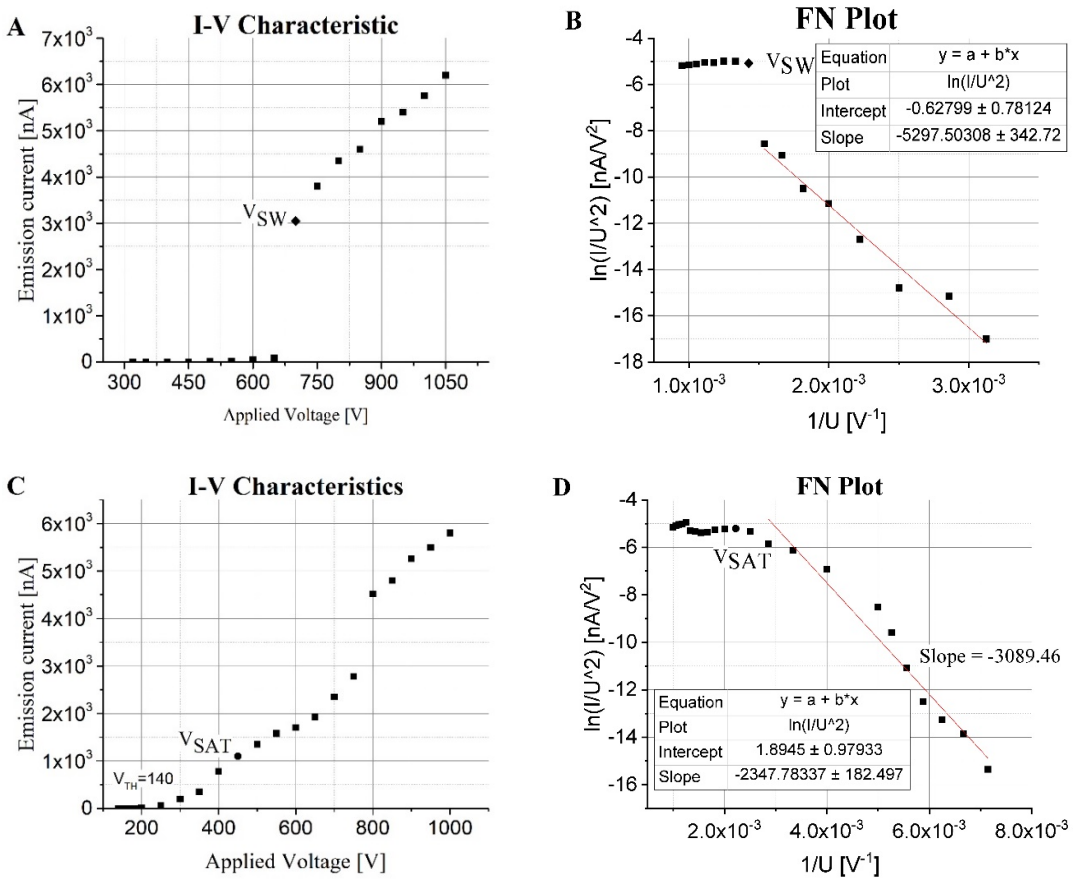

FIG. 8. SWCNT-21 before cooling process with increasing applied voltage. (A) I-V Characteristics. (B) FN plot. When applied voltage decreased (C) I-V Characteristics. (D) FN Plot.

After applying the cooling process, we slowly increased the applied voltage on the tip until the emission current has been initiated at an applied voltage value of (230 V), with an emission current value of (250 pA). "Switch-on" phenomenon appeared at (V_{SW} = 1000 V, ISW = 3.6×10^3 nA). By decreasing the applied voltage, emission current remains in the (μA) range until the applied voltage reached (V_{SAT} = 500 V, I_{SAT} = 1.0×10^3 nA). By further decreasing the applied voltage, the emission current vanishes at (V_{TH} = 20 V), with an emission current value (I_{TH}=50 pA). Figure (9) shows the I-V Characteristics, with related FN plots. It can be noticed by comparing the I-V characteristics before and after the cooling process that there is an emission current fluctuation being increased after the cooling process. It can also be noted that from Fig. 10, the emission current pattern gets distributed over the screen as an effect of the cooling process. Figs. (10 A, B and C) show the emission current images before the cooling process, where they are more concentrated than those after the cooling process. Figs. (10 D, E and F) show the emission current images after the cooling process.

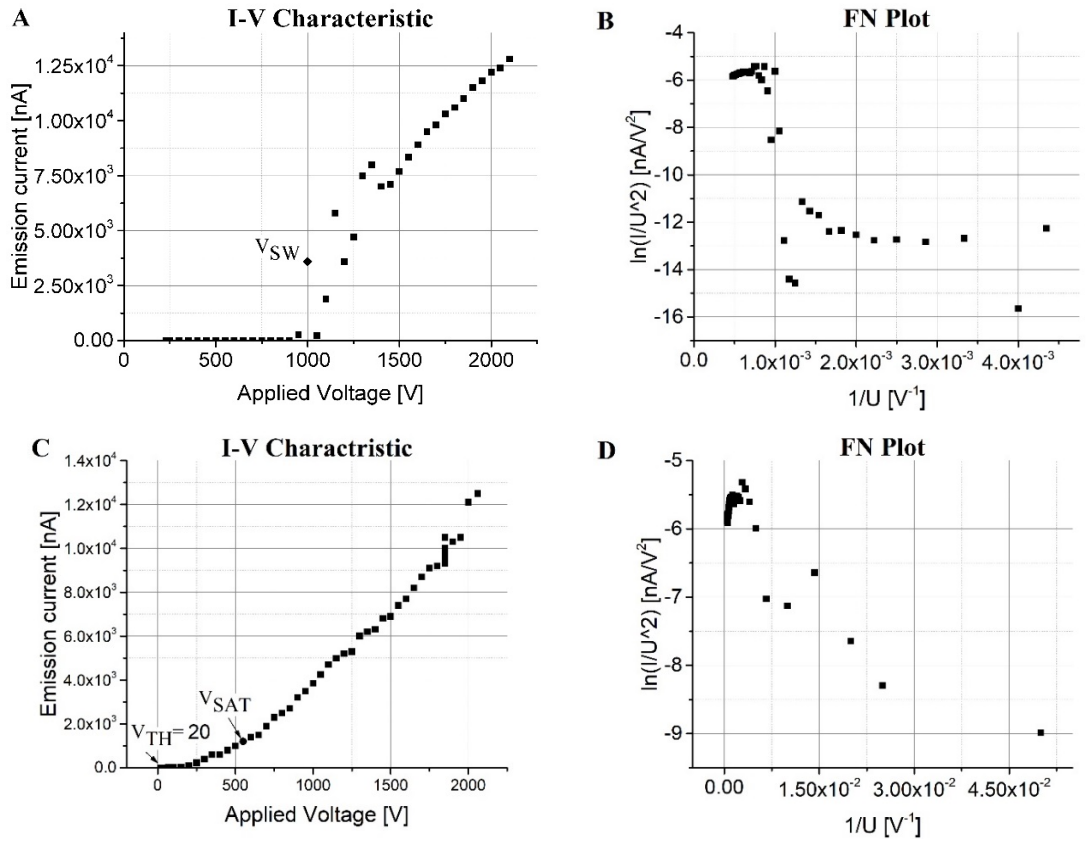

FIG. 9. (SWCNT-21). After cooling process. As applied voltage increased (A) I-V Characteristic and (B) FN plot. As applied voltage decreased (C) I-V Characteristics. (B) FN Plot.

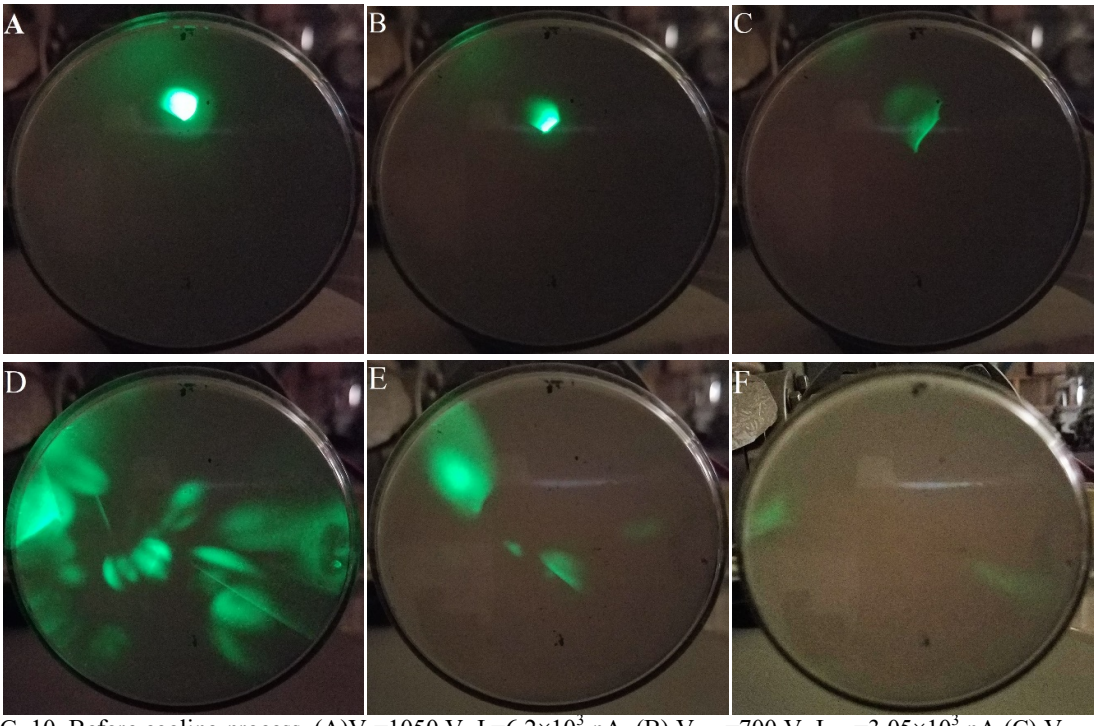

FIG. 10. Before cooling process. (A)V =1050 V, I =6.2×10^3 nA. (B) V_{SW} =700 V, I_{SW} =3.05×10^3 nA (C) V_{SAT} = 450 V, I_{SAT} = 1.1×10^3 nA. After cooling process. (D) V =1550 V, I =7.4×10^3 nA. (E) V_{SW} =1000 V, I_{SW} = 3.6×10^3 nA. (F) V_{SAT} =500 V, I_{SAT} =1.0×10^3 nA.

By comparing Fig. 8 with Fig. 9, it can be noticed that there is an occurrence of emission current fluctuation after performing the cooling process. Additionally, the switch-on phenomenon has occurred at higher voltage values after applying the cooling process. Also, the saturated region extends down to a higher voltage value, but the threshold voltage would have a lower value (V_{TH} = 20 V) after applying cooling process.

Conclusions

SWCNT emitters have been prepared by employing a drawing method using a glass puller technique. The effects of the relaxation and cooling processes on the FEE have been studied from plotting the I-V characteristics and the FN plots along with the emission current images obtained. The relaxation process has shown to have a significant impact on the FEE, where it causes a reduction in the applied voltage values required for the "switch-on" phenomenon to take place. Additionally, the saturation region extends down to a lower voltage value and can also enhance the emission current pattern, where it causes it to become more focused and concentrated.

The cooling process affects the FEE mechanism, where V_{SW} and V_{SAT} have increased after the cooling process. The most remarkable impact of the cooling process on FEE is the lowering of the V_{TH} value significantly, which is the lowest applied voltage value that can yield the lowest emission current. Moreover, the cooling process resulted in having the emission current pattern to become non-uniformly distributed over the screen. Also, a constant resistance has been observed at the emitter tip, where this can be indicated from the linear behavior that appears in the I-V plots.

References

[1] Parveen, S., Kumar, A., Husain, S. and Husain, M., Physica B: Condensed Matter, 505 (2017) 1.

[2] Stratton, R., Proceedings of the Physical Society. Section B, 68 (10) (1955) 746.

[3] Arkhipov, A.V., Gabdullin, P.G., Gnuchev, N.M., Davydov, S.N., Krel, S.I. and Loginov, B.A., St. Petersburg Polytechnical University Journal: Physics and Mathematics, 1 (1) (2015) 47.

[4] Beams, J.W., Physical Review, 44 (10) (1933) 803.

[5] Vyšinka, M., Vaverka, J., Pavlu, J., Nemecek, Z. and Šafránková, J., WDS'12 Proceedings of Contributed Papers, Part 2 (2012) 151.

[6] Rinzler, A.G., Hafner, J.H., Nikolaev, P., Nordlander, P., Colbert, D.T., Smalley, R.E., Lou, L., Kim, S.G. and Tomanek, D., Science, 269 (5230) (1995) 1550-3.

[7] Sun, Y., Shin, D.H., Yun, K.N., Hwang, Y.M., Song, Y., Leti, G., Jeon, S.-G., Kim, J.-I., Saito, Y. and Lee, C.J., AIP Advances, 4 (7) (2014) 077110.

[8] Cheng, Y. and Zhou, O., Comptes Rendus Physique, 4 (9) (2003) 1021.

[9] Hata, K., Takakura, A. and Saito, Y., Ultramicroscopy, 95 (2003) 107.

[10] Iijima, S., Nature, 354 (6348) (1991) 56.

[11] Iijima, S. and Ichihashi, T., Nature, 363 (6430) (1993) 603.

[12] Peng, J., Li, Z., He, C., Deng, S., Xu, N., Zheng, X. and Chen, G., Physical Review B, 72 (23) (2005) 235106.

[13] Dean, K.A. and Chalamala, B.R., Applied Physics Letters, 75 (19) (1999) 3017.

[14] Chen, C.-W., Lee, M.-H. and Clark, S.J., Applied Surface Science, 228 (1) (2004) 143.

[15] Chau, R., Datta, S., Doczy, M., Doyle, B., Jin, B., Kavalieros, J., Majumdar, A., Metz, M. and Radosavljevic, M., IEEE Transactions on Nanotechnology, 4 (2) (2005) 153.

[16] Choi, W.B., Chung, D.S., Kang, J.H., Kim, H.Y., Jin, Y.W., Han, I.T., Lee, Y.H., Jung, J.E., Lee, N.S., Park, G.S. and Kim, J.M., Applied Physics Letters, 75 (20) (1999) 3129.

[17] Lin, H., Zhu, H., Guo, H. and Yu, L., Materials Research Bulletin, 43 (10) (2008) 2697.

[18] Baughman, R.H., Zakhidov, A.A. and de Heer, W.A., Science, 297 (5582) (2002) 787.

[19] Fowler, R.H. and Nordheim, L.W., Proceedings of the Royal Society of London, Series A: Mathematical, Physical and Engineering Sciences, 119 (781) (1928) 137.

[20] Forbes, R., Deane, J., Fischer, A. and Mousa, M., Jordan J. Phys., 8 (3) (2015) 125.

[21] Mousa, M., Surface Science, 246 (1) (1991) 79.

[22] Al-Qudah, A., Mousa, M. and Fischer, A., IOP Conference Series: Materials Science and Engineering, 92 (1) (2015) 012021.

[23] Kim, C., Choi, Y.S., Lee, S.M., Park, J.T., Kim, B. and Lee, Y.H., Journal of the American Chemical Society, 124 (33) (2002) 9906.

[24] Oki, H., Kinoshita, A., Takikawa, T., Kim, W.S., Murakami, K., Abo, S., Wakaya, F. and Takai, M., Journal of Vacuum Science & Technology: B - Microelectronics and Nanometer Structures, 27 (2) (2009).

[25] Mousa, M.S., Al-Akhras, M.-A. and Daradkeh, S.I., Jordan J. Phys., 11 (1) (2018) 17.

[26] Latham, R.V. and Mousa, M.S., Journal of Physics D: Applied Physics, 19 (4) (1986) 699.

[27] Minoux, E., Groening, O., Teo, K.B.K., Dalal, S.H., Gangloff, L., Schnell, J.-P., Hudanski, L., Bu, I.Y.Y., Vincent, P., Legagneux, P., Amaratunga, G.A.J. and Milne, W.I., Nano-Letters, 5 (11) (2005) 2135.

[28] Chen, L.F., Song, H., Cao, L.Z., Jiang, H., Li, D.B., Guo, W.G., Liu, X., Zhao, H.F. and Li, Z.M., Journal of Applied Physics, 106 (3) (2009) 033703.